This article was downloaded by: [Tomsk State University of Control Systems and Radio]
On: 21 February 2013, At: 11:49
Publisher: Taylor & Francis
Informa Ltd Registered in England and Wales Registered Number: 1072954
Registered office: Mortimer House, 37-41 Mortimer Street, London W1T 3JH, UK

Molecular Crystals and Liquid Crystals
Publication details, including instructions for authors and subscription information:
http://www.tandfonline.com/loi/gmcl16

ESR Line Shape Study of Two Nematic Liquid Crystals

R. Rai [a] , S. R. Singhal [a] , S. K. Gupta [a] & V. G. Bhide [a]

[a] Division of Specialized Techniques, National Physical Laboratory, New Delhi, 110012, India
Version of record first published: 28 Mar 2007.

To cite this article: R. Rai , S. R. Singhal , S. K. Gupta & V. G. Bhide (1982): ESR Line Shape Study of Two Nematic Liquid Crystals, Molecular Crystals and Liquid Crystals, 87:3-4, 173-186

To link to this article: http://dx.doi.org/10.1080/00268948208084440

PLEASE SCROLL DOWN FOR ARTICLE

Full terms and conditions of use: http://www.tandfonline.com/page/terms-and-conditions

This article may be used for research, teaching, and private study purposes. Any substantial or systematic reproduction, redistribution, reselling, loan, sub-licensing, systematic supply, or distribution in any form to anyone is expressly forbidden.

The publisher does not give any warranty express or implied or make any representation that the contents will be complete or accurate or up to date. The accuracy of any instructions, formulae, and drug doses should be independently verified with primary sources. The publisher shall not be liable for any loss, actions, claims, proceedings, demand, or costs or damages

whatsoever or howsoever caused arising directly or indirectly in connection with or arising out of the use of this material.

Downloaded by [Tomsk State University of Control Systems and Radio] at 11:49 21 February 2013

Mol. Cryst. Liq. Cryst., 1982, Vol. 87, pp. 173–186
0026-8941/82/8703-0173$06.50/0
© 1982 Gordon and Breach, Science Publishers, Inc.
Printed in the United States of America

Downloaded by [Tomsk State University of Control Systems and Radio] at 11:49 21 February 2013

ESR Line Shape Study of Two Nematic Liquid Crystals

R. RAI, S. R. SINGHAL, S. K. GUPTA and V. G. BHIDE

Division of Specialized Techniques, National Physical Laboratory, New Delhi-110012, India

(*Received October 21, 1981; in final form December 16, 1981*)

Electron spin-resonance (ESR) measurements of the spin-probe 17β-hydroxy-4,4'-dimethyl spiro[5α-androstane-3,2-oxazolidine]-3'-yloxyl in the liquid crystals 4-*n*-Amylacetophenon 0-(4-*n*-heptyl benzoyl)-oxime [AAHBO] and 4-*n*-Butoxyphenyl hexyl benzoate [BPHB] are reported in isotropic and nematic phases. On the basis of the temperature variation of ESR line width, an extra, solid to solid, phase transition is observed in BPHB. The theory of Polnaszek, Bruno and Freed (PBF) appropriate for anisotropic viscosity diffusion is used to analyze the ESR spectra and thereby to determine the values of the order parameter, the rotational diffusion tensor and the correlation time at different temperatures for the two liquid crystals. The analysis shows that the slowly relaxing local structure mechanisms (SRLS) is active in slow tumbling region specially in AAHBO.

1. INTRODUCTION

The ESR study of the rotation motion of the spin-probes is a well known technique to provide information about the structure and molecular dynamics of the host liquid crystals.[1-3] The motional narrowing condition $|\mathcal{H}_1(\Omega)|\tau_R \leq 1$, where $\mathcal{H}_1(\Omega)$ is rotational dependent perturbation in the spin-Hamiltonian and τ_R is the rotational correlation time, is not valid in the case of viscous liquid crystals and large probe molecules.[4-6] A slow motional analysis, therefore, is the appropriate approach to analyze the ESR spectra in these cases. The PBF theory[6] is valid for both the motional narrowing and the slow tumbling region. The present paper deals with ESR study of an androstane nitroxide derivative, as a probe, in two nematic liquid crystals AAHBO and BPHB their detailed chemical formulas are given in Section 2.1. The spectra are analyzed using PBF theory.

The analysis of the ESR spectra results in the determination of the order parameter S_z, the rotation diffusion tensor **R** and the correlation

time τ_R. The temperature variation of correlation time τ_R shows a good Arhenius behavior for both the samples. The Arhenius plot, that is the ln τ_R versus $1/T$ curve, is used to calculate the activation energy.

2. MATERIALS

The chemical formulas and transition temperatures[7] of liquid crystals used in the present study are as follows:

(i) 4-*n*-Amylacetophenon-0-(4-*n*-heptyl benzoyl)-oxime (AAHBO)

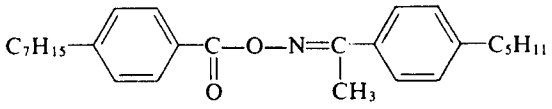

$$\text{Solid} \xrightarrow{30.0^\circ C} \text{Nematic} \xrightarrow{68.5^\circ C} \text{Isotropic}$$

(ii) 4-*n*-Butoxy phenyl hexyl benzoate (BPHB)

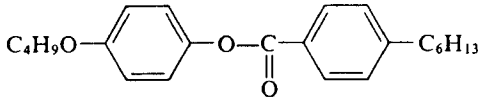

$$\text{Solid} \xrightarrow{43.5^\circ C} \text{Nematic} \xrightarrow{49.0^\circ C} \text{Isotropic}$$

These samples were acquired by Dr. Bahadur of this laboratory from Prof. Demus of Martin Luther University, G.D.R.

The androstane nitroxide paramagnetic probe was purchased from M/s. Syva, Palo Alto, California, U.S.A. Its chemical formula is

17β-Hydroxy-4,4'-dimethyl spiro[5α-androstane 3,2'-oxazolidine]-3'-yloxyl

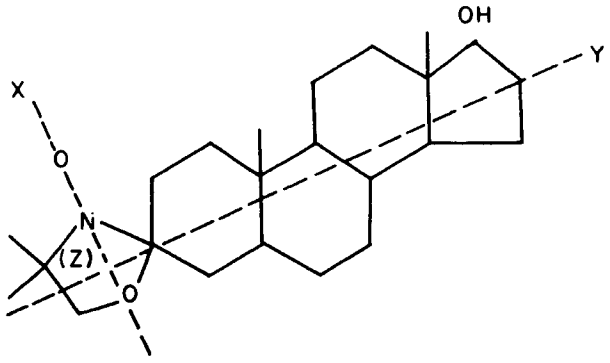

Downloaded by [Tomsk State University of Control Systems and Radio] at 11:49 21 February 2013

This probe is a long cylindrical molecule with symmetric axis parallel to N—O bond.[8] It is rigid and stable over the entire range of temperture required for our ESR study.

Downloaded by [Tomsk State University of Control Systems and Radio] at 11:49 21 February 2013

3. ESR MEASUREMENTS

The samples for ESR study were prepared by heating the mixture of the required liquid crystal with a small amount of the probe. The concentration of the probe molecules in liquid crystal solvent was less than 0.1% below which no further narrowing of the resonance lines was observed. The probe molecules were found to be perfectly soluble in both the liquid crystals. ESR measurements were carried out using Varian V-4502, X-band (9.3 GHz/Sec) ESR spectrometer and 100 KHz magnetic field modulation. The spectra were recorded at different temperatures between room temperature and 80°C range, using the Varian V-4547 variable temperature accessory. A separate copper-constantan thermocouple was attached to the sample tube to check the temperature of the sample. The sample was filled up to 5 mm height in quartz tube of internal diameter of 2 mm to minimize the thermal gradient. Temperature could be held constant to within ±0.1°C.

The ESR spectra were recorded in cooling cycle for both the samples. Sufficient time was given at each temperature to stabilize the temperature particularly near transition temperatures. Three line spectra, characteristic of a nitroxide probe ($S = \frac{1}{2}, I = 1$) were obtained in all the mesophases of the two liquid crystals (Figures 1, 2). The variation of the line width as a function of temperature for both the samples is shown in Figure 3. It is seen that the abrupt change in line width at Isotropic–Nematic transition temperature is a common feature for all the curves. In the liquid crystal BPHB, the ESR spectrum was distorted at 26°C which shows that the solidification of the sample has started. The transition from nematic to solid is not observed in AAHBO probably because of supercooling.

A preliminary DSC measurement by one of us[9] on these samples has shown that liquid crystal AAHBO always exhibits usual two transitions, whereas for the liquid crystal BPHB, quenched at a rate of 8°C/min or more, three peaks occur (instead of two) in the heating cycle thermogram. Therefore, to understand the nature of this additional transition in BPHB, we performed the ESR measurements on this sample in the heating cycle also after the sample was quenched from isotropic state to supercooled solid. The result is shown in Figures 4 and 5 and is discussed in Section 5.3.

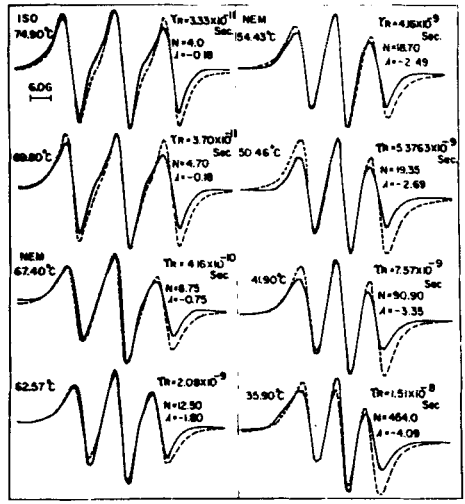

FIGURE 1 ESR lineshape simulations for the liquid crystal AAHBO using PBF theory. --------- Theoretical ——— Experimental.

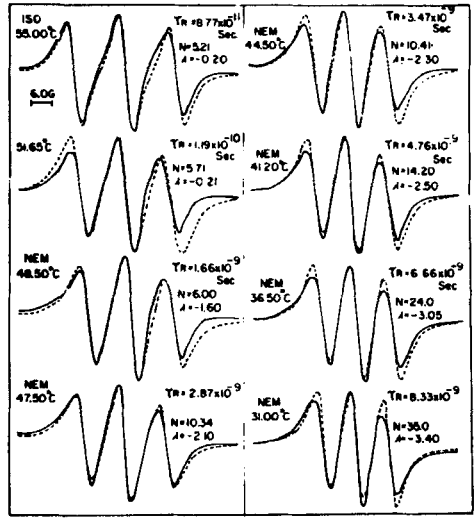

FIGURE 2 ESR lineshape simulations for the liquid crystal BPHB using PBF theory. --------- Theoretical ——— Experimental.

Downloaded by [Tomsk State University of Control Systems and Radio] at 11:49 21 February 2013

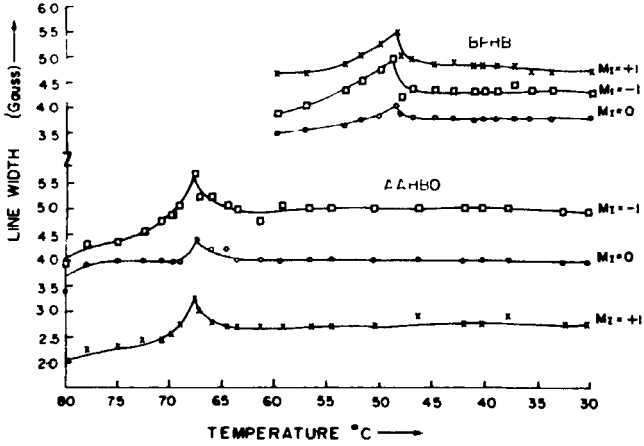

FIGURE 3 Variation of ESR line width with temperature.

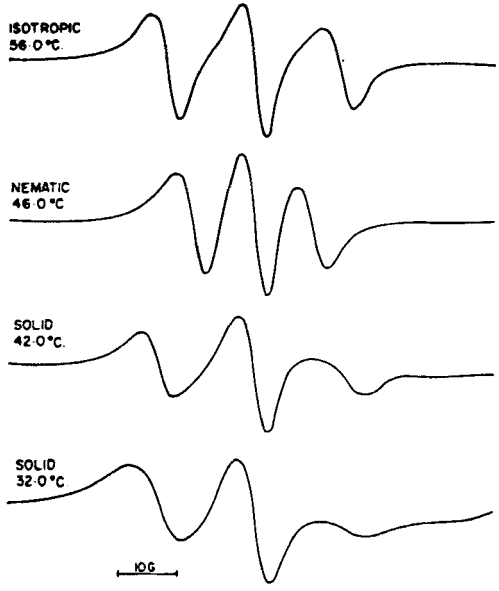

FIGURE 4 Heating cycle ESR spectra of quenched BPHB sample.

Downloaded by [Tomsk State University of Control Systems and Radio] at 11:49 21 February 2013

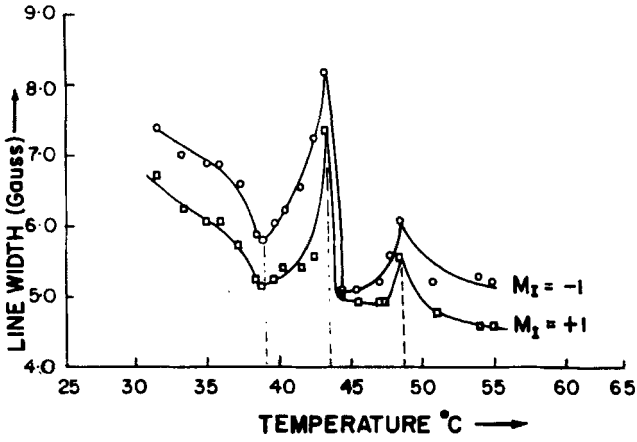

FIGURE 5 Variation of heating cycle ESR linewidth for quenched BPHB sample.

4. THE ESR LINE SHAPE ANALYSIS

The PBF theory[6] is based upon the Stochastic Louville method of analysis of ESR spectra of a Brownian particle undergoing an anisotropic rotational diffusion under a mean restoring potential, the potential of the restoring torque. The basic result of this theory is that the unsaturated microwave absorption $A_j(\omega)$ of the jth transition is given by

$$A_j(\omega) = \mathrm{Im} \int d\Omega \, \bar{Z}_j(\Omega, \omega) P_0^{1/2}(\Omega) \tag{1}$$

Here $P_0(\Omega)$ is the Boltzman equilibrium distribution of the probe for orientation Ω, specified by the Eulerian angles $(\varphi, \theta, \vartheta)$, and $\bar{Z}_j(\Omega, \omega)$ satisfies the equation[6]

$$\{[\omega + \mathcal{H}_0^x + \mathcal{H}_1(\Omega)^x - i\bar{\Gamma}_\Omega]\bar{Z}(\Omega, \omega)\}_j = \frac{\omega_\gamma}{2} P_0^{-1/2}(\Omega)[S_-^x \rho_0]_j \tag{2}$$

A^x represents the super operator of A such that $A^x B = AB - BA$. $\mathcal{H}_0$ and $\mathcal{H}_1(\Omega)$ are respectively isotropic and orientational dependent parts of the spin-Hamiltonian,[4] and $\bar{\Gamma}_\Omega$ is the symmetrized Markoff operator.[6] ω_γ is frequency of the rf field and ρ_0 is the equilibrium spin-density matrix.[4] We have considered here a simple one term Maire Saupe potential

$$U(\theta) = \epsilon \cos^2 \theta \tag{3}$$

Downloaded by [Tomsk State University of Control Systems and Radio] at 11:49 21 February 2013

where θ is the angle between the molecular Z-axis (the N—O bond direction) of the probe and director axis of the host. For a cylindrical nitroxide probe, the equilibrium orientation is $\theta_{eq} = \pi/2$, while P_0 is given by

$$P_0(\theta) = \exp(\lambda \cos^2 \theta) \Big/ \int_0^{\pi} d\theta \sin \theta \exp(\lambda \cos^2 \theta) \tag{4}$$

with

$$\lambda = -\frac{\epsilon}{kT} \tag{5}$$

$\tilde{Z}_j(\Omega, \omega)$ can be expanded as sum of products of orientational dependent and independent terms as follows:[6]

$$\tilde{Z}_j(\Omega, \omega) = \sum_{L',K',M'} \sqrt{2L'+1}\, D^{L'}_{K',M'}(\Omega)[C^{L'}_{K',M'}(\omega)]_j \tag{6}$$

where $D^{L'}_{K',M'}(\Omega)$ are Wigner rotational matrices. Substituting Eqs. (4) and (5) in Eq. (2), premultiplying Eq. (2) with $\sqrt{2L+1}\, D^{L}_{K,M}(\Omega)$ integrating it with respect to Ω and utilizing high temperature approximation in the right hand side we arrive at

$$(\omega - \omega_j - iT_2^{-1})[C^L_{K,M}(\omega)]_j + \sum_{L'} \sqrt{(2L+1)(2L'+1)}$$

$$\times \langle D^L_{K,M}(\Omega)|\, \mathcal{H}_1(\Omega)^x - i\tilde{\Gamma}_\Omega |\, D^{L'}_{K',M'}(\Omega)\rangle [C^{L'}_{K',M'}(\omega)]_j$$

$$= \frac{\hbar \omega_j \omega_\gamma}{4kT} \sqrt{2L+1}\, \langle D^L_{K,M}(\Omega)|\, P_0^{1/2}(\theta)\rangle \delta_{K,0}\delta_{M,0} \tag{7}$$

In Eq. (7) $\hbar\omega_j$ is the energy difference under $\mathcal{H}_0$ between two levels involved in jth transition and T_2^{-1} is introduced arbitrarily to take into account the rotational invariant line width. $\mathcal{H}_1(\Omega)^x$ and $\tilde{\Gamma}_\Omega$ Eq. (7) are simultaneously diagonalized to achieve solution for the coefficient $[C^L_{00}(\omega)]_j$. The total absorption $A(\omega)$ is obtained by summing Eq. (1) with respect to j and utilizing Eqs. (4) and (6).

$$A(\omega) = \mathrm{Im} \sum_L \sum_j (2L+1)^{1/2} \langle D^L_{00}(\theta)|\, P_0^{1/2}(\theta)\rangle [C^L_{00}(\omega)]_j \tag{8}$$

The suffix j in Eqs. (2) and (7) stand for all the transitions while in Eq. (8) the contribution comes only from three allowed transitions corresponding to the three m_I values 1, 0, −1.

The symmetrized Markoff operator $\tilde{\Gamma}_\Omega$ appropriate for anisotropic

Downloaded by [Tomsk State University of Control Systems and Radio] at 11:49 21 February 2013

viscosity and the pseudopotential given in Eq. (3) is utilized. It involves[6,10] the parameters λ, $R_\parallel$ and $R_\perp$. $R_\parallel$ and $R_\perp$ are the components of rotational diffusion tensor **R**, parallel and perpendicular to the director axis respectively. In $\mathcal{H}_1(\Omega)$ the terms up to pseudosecular[4] are considered and the axially symmetric magnetic and hyperfine tensors are employed.

Equation (8) is equivalent to a set of simultaneous coupled equations whose order depends upon the values of L, L' (Appendix). We have limited $L, L' \leqslant 6$ and only even values of L, L' are required. The resulting matrix is solved numerically on IBM 360 computer for different set of values of the involved parameters. The values of these parameters at different temperatures obtained for the best fit with the experimental ESR derivative curve are shown in Figures 1 and 2. These figures compare the simulated ESR spectra with the experimental curves at different temperatures in isotropic and nematic regions.

5. RESULTS AND DISCUSSION

5.1. Order parameter

An orientational order parameter S_Z is defined as

$$S_Z = \frac{1}{2}\langle 3\cos^2\theta - 1\rangle = \int_0^\pi d\theta \sin\theta \frac{1}{2}(3\cos^2\theta - 1)P_0(\theta) \quad (9)$$

S_Z obviously involves the parameter λ. Since g-tensor for androstane is very nearly isotropic,[11] the order parameter S_Z in the motional narrowing region can also be obtained by using the relation[12]

$$S_Z = \frac{1}{2}[\langle a\rangle - a]/(a - a_\perp) \quad (10)$$

where the isotropic hyperfine parameter a was obtained from the isotropic spectrum. $\langle a\rangle$ was measured from the ESR spectrum in mesophase and $a_\perp = a_y$ is the component of hyperfine coefficient perpendicular to the symmetry axis (N—O bond direction) of the probe. The order parameter calculated using expressions (9) and (10) are compared in Figure 6. The values from the two expressions coincide near isotropic nematic transition temperature but differ increasingly as the temperature decreases. This is because of the fact that the expression (10) is not valid in the slow tumbling region. Expression (9) however combined with Eq. (10) can be used to suggest approximate value of λ which is then refined to provide best simulation of the ESR spectra.

Downloaded by [Tomsk State University of Control Systems and Radio] at 11:49 21 February 2013

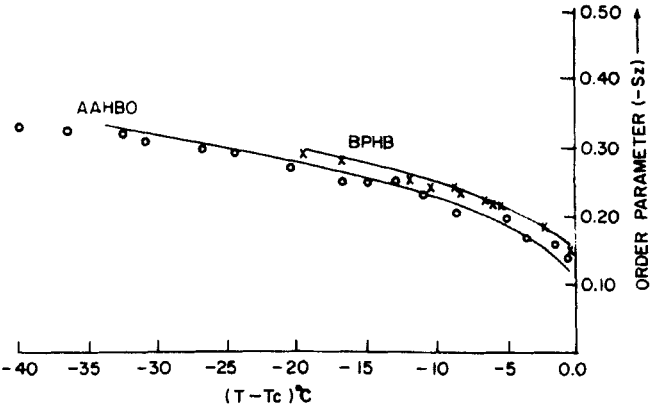

FIGURE 6 Temperature variation of order parameter for nematic liquid crystals. XXX and OOO are experimental points while the curve results from ESR shape analysis using PBF theory.

5.2. Diffusion parameter and correlation time

The effect of anisotropic-viscosity rotational diffusion can be best studied in terms of the anisotropic parameter $N = R_{\parallel}/R_{\perp}$ and the rotational correlation time $\tau_R = 1/6R_{\perp}$. In the isotropic phase in both the liquid crystals, N nearly remains constant at ≈ 5. This is expected since in the isotropic phase N is mainly a function of the geometry of the probe.[10] With the onset of nematic phase $R_{\perp}$ decreases continuously with decreasing temperature while $R_{\parallel}$ first decreases, though at a slower rate than $R_{\perp}$, and then increases with incipient slow tumbling region ($\tau_R \geqslant 10^{-9}$ sec). As a result in the nematic region N increases with decreasing temperature first slowly but acquires very high values for $\tau_R \geqslant 10^{-9}$ sec. The decrease of $R_{\parallel}$ and $R_{\perp}$ is reasonable since the effect of decreasing temperature is to quench the rotational motion. Moreover the onset of ordering causes preferentially more quenching of rotational motion around an axis perpendicular to the director than the rotation around the director axis itself and hence $R_{\perp}$ decreases faster than $R_{\parallel}$. The increase of $R_{\parallel}$ with the incipient slow tumbling region, however, is an anomolous behavior. Similar results are also obtained in the case of PD-Tempone (a nitroxide probe) in various liquid crystalline solvents.[10,14] These apparently implausible results are explained by invoking a slowly relaxing local structure (SRLS) mechanism, in which the rod like solvent molecules present a persistent local structure for the probe, which relaxes on a time scale much slower than the reorientation of the probe. This SRLS mechanism, which makes the diffusion coefficient frequency dependent, seems to be important in the

Downloaded by [Tomsk State University of Control Systems and Radio] at 11:49 21 February 2013

present cases also specially in the liquid crystal AAHBO (Figure 7). These refinements however are not attempted in the present paper.

In the isotropic phase the correlation time τ_R is of the order of 10^{-10} sec in AAHBO and 10^{-11} sec in BPHB. At isotropic-nematic transition temperature τ_R abruptly increases. In the mesophase ln τ_R versus $1/T$ curve shows a good Arhenius behavior for both the samples (Figure 8). From the slope of the curves the activation energies are calculated to be 11.38 kcal/mole for AAHBO and 11.88 kcal/mole for BPHB. These values are of the same order as the experimental activation energies for various other liquid crystals.[15]

5.3. Solid to solid phase transition in BPHB

The heating cycle ESR spectra of a quenched sample of BPHB are shown in Figure 4. The ESR lines were not resolved properly up to 30°C. Beyond this temperature the line widths show abrupt changes at 39°C, 44°C and 49°C (Figure 5), which confirms the three phase transitions observed in DSC measurements. As a first guess one may think of an extra transition at 39°C to be from a supercooled liquid to a glassy phase.[16] The ESR spectra below 44°C, however do not change when the sample is rotated with respect to the magnetic field. Even the spectra of samples quenched in high magnetic field ($\approx$10 KG) do not show any angular dependence in the temperature range 30°C–44°C. Also the separation of the low and high field hyperfine extrema is about the same as in the isotropic phase (Figure 4), which indicates that no ordering takes place in the sample.[11] The lack of angular dependence of the spectra and the lack of ordering in the sample clearly rules out the possibility of any glass phase[16,17] above 30°C.

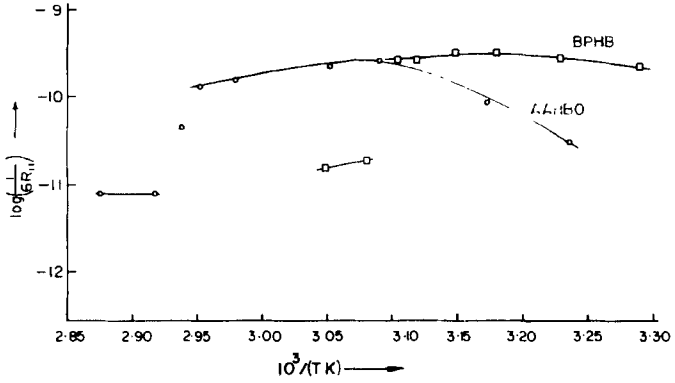

FIGURE 7 Temperature variation of rotational diffusion tensor component $R_{\parallel}$ (sec^{-1}).

Downloaded by [Tomsk State University of Control Systems and Radio] at 11:49 21 February 2013

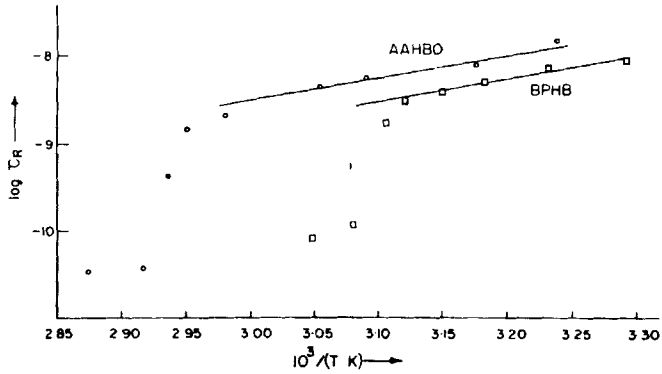

FIGURE 8 Temperature variation of rotational correlation time τ_R (sec/rad) in logarithmic scale.

The extreme broadening of the spectra at 44°C may be regarded as the motional broadening in the near rigid limit due to motional effects which carry the spin-probe between different orientations corresponding to different resonance frequencies.[18] Above this temperature the line width narrows as the increased molecular motion averages out the above broadening effect. Below this temperature the convenient method of Mason and Freed,[18] applicable for near rigid limit, is used to estimate the reorientational correlation time τ_R. τ_R just below 44°C is of the order of 10^{-7} sec and increases to 10^{-6} sec as the temperature is further lowered. This indicates that the sample is in solid phase in 30°C–44°C temperature range. The transition at 39°C, therefore, is between two solid phases. Further work is in progress to elucidate more details about the nature of this solid to solid phase transition.

Acknowledgments

Authors are thankful to Prof. D. Demus and Dr. B. Bahadur for providing the liquid crystal samples. Valuable help in computation by Dr. S. K. Jain is very gratefully acknowledged. One of us (S.R.S.) acknowledges the financial support from U.G.C., New Delhi.

References

1. G. R. Luckhurst, in *Electron Spin Relaxation in Liquids*, Ed. L. T. Muus and P. W. Atkins, Plenum Press, p. 411 (1972).
2. J. Seeling, in *Spin Labelling, Theory and Applications*, Ed. L. J. Berliner, Academic Press, New York (1976).

Downloaded by [Tomsk State University of Control Systems and Radio] at 11:49 21 February 2013

3. S. R. Singhal, S. K. Gupta and V. G. Bhide, *Proc. of Int. Conf. on Liquid Crystals,* Bangalore (India), Ed. S. Chandrashekhar, Hyden and Sons Ltd. (London), p. 473 (1980).
4. J. H. Freed, G. V. Bruno and C. F. Polnaszek, *J. Phys. Chem.*, **75**, 22 (1971).
5. S. A. Goldman, G. V. Bruno, C. F. Polnaszek and J. H. Freed, *J. Chem. Phys.*, **56**, 716 (1972).
6. C. F. Polnaszek, G. V. Bruno and J. H. Freed, *J. Chem. Phys.*, **8**, 3185 (1973).
7. D. Demus, H. Demus and H. Zaschle, Flussige Kristalle in Tabellen, pp. 64, 139, VEB Deutscher Verlag für Grundstoffindustrie, Lepzing (1974).
8. E. Meirovitch and Z. Luz, *Mol. Phys.*, **30**, 1589 (1975).
9. S. R. Singhal, Ph.D. Thesis (Delhi University) in preparation.
10. C. F. Polnaszek and J. H. Freed, *J. Phys. Chem.*, **79**, 2283 (1975).
11. F. Pusnik, M. Schara and M. Sentjurc, *J. de Physique,* **36**, 665 (1975).
12. N. M. Atherton, Electron Spin Resonance, Ellis Horwood, Chichester (U.S.A.), 1973.
13. J. H. Freed, *J. Chem. Phys.*, **41**, 2077 (1964).
14. J. S. Hwang, K. V. S. Rao and J. H. Freed, *J. Phys. Chem.*, **80**, 1490 (1976).
15. P. J. Flanders, *Mol. Cryst. Liq. Cryst.*, **29**, 19 (1974).
16. J. E. Lydon and J. O. Kessler, *J. Physique (Paris)*, **36**, C1-153 (1975).
17. A. E. Stillman, L. L. Jones, R. N. Schwartz and B. L. Bales, 1978, *Liquid Crystals and Ordered Fluids,* Vol. 3, edited by J. F. Johnson and R. S. Poster (Plenum Press), p. 399.
18. R. P. Mason and J. H. Freed, *J. Phys. Chem.*, **78**, 1321 (1974).

Appendix

The coupled equations involving various $C^{L}_{KM}(j)$'s as unknown are written with the help of Refs. 5 and 6 and are described below for the sake of completeness.

$$[(\omega - \omega_0 + 2b) - i(T_2^{-1} + \tau^{-1}_{L,0})]\,\bar{C}^{L}_{K,0}(1) - \sum_{L'} N(LL')\Big((F + D')\begin{pmatrix} L & 2 & L' \\ -K & 0 & K \end{pmatrix}\begin{pmatrix} L & 2 & L' \\ 0 & 0 & 0 \end{pmatrix}\bar{C}^{L'}_{K,0}(1) + \frac{D}{\sqrt{2}}\begin{pmatrix} L & 2 & L' \\ -K & 0 & K \end{pmatrix}\begin{pmatrix} L & 2 & L' \\ 0 & 1 & -1 \end{pmatrix}[\bar{C}^{L'}_{K,-1}(5) - \bar{C}^{L'}_{K,1}(4)] - iR_\perp G^{L'}_{K,0}(1)\Big) = \delta_{K,0}\,\delta_{M,0}\,X_1 I_L \quad \text{(A1)}$$

$$[(\omega - \omega_0) - i(T_2^{-1} + \tau^{-1}_{L,0})]\,\bar{C}^{L}_{K,0}(2) - \sum_{L'} N(LL')\Big(F\begin{pmatrix} L & 2 & L' \\ -K & 0 & K \end{pmatrix}\begin{pmatrix} L & 2 & L' \\ 0 & 0 & 0 \end{pmatrix}\bar{C}^{L'}_{K,0}(2) + \frac{D}{\sqrt{2}}\begin{pmatrix} L & 2 & L' \\ -K & 0 & K \end{pmatrix}\begin{pmatrix} L & 2 & L' \\ 0 & 1 & -1 \end{pmatrix}\{[\bar{C}^{L'}_{K,-1}(5) - \bar{C}^{L'}_{K,1}(4)] + [\bar{C}^{L'}_{K,-1}(7) - \bar{C}^{L'}_{K,1}(6)]\} - iR_\perp G^{L'}_{K,0}(2)\Big) = \delta_{K,0}\,\delta_{M,0}\,X_2 I_L \quad \text{(A2)}$$

Downloaded by [Tomsk State University of Control Systems and Radio] at 11:49 21 February 2013

$$[(\omega - \omega_0 - 2b) - i(T_2^{-1} + \tau_{L,0}^{-1})]\,\bar{C}^{L}_{K,0}(3)$$
$$- \sum_{L'} N(LL')\Big((F - D')\begin{pmatrix} L & 2 & L' \\ -K & 0 & K \end{pmatrix}\begin{pmatrix} L & 2 & L' \\ 0 & 0 & 0 \end{pmatrix}\bar{C}^{L'}_{K,0}(3)$$
$$+ \frac{D}{\sqrt{2}}\begin{pmatrix} L & 2 & L' \\ -K & 0 & K \end{pmatrix}\begin{pmatrix} L & 2 & L' \\ 0 & 1 & -1 \end{pmatrix}[\bar{C}^{L'}_{K,-1}(7) - \bar{C}^{L'}_{K,1}(6)] - iR_\perp G^{L'}_{K,0}(3)\Big)$$
$$= \delta_{K,0}\,\delta_{M,0}\,X_3 I_L \quad \text{(A3)}$$

$$[(\omega - \omega_0 + b) - i(T_2^{-1} + \tau_{L,1}^{-1})][\bar{C}^{L}_{K,1}(4) - \bar{C}^{L}_{K,-1}(5)]$$
$$+ \sum_{L'} N(LL')\Big[\Big(F + \frac{D'}{2}\Big)\begin{pmatrix} L & 2 & L' \\ -K & 0 & K \end{pmatrix}\begin{pmatrix} L & 2 & L' \\ -1 & 0 & 1 \end{pmatrix}[\bar{C}^{L'}_{K,1}(4) - \bar{C}^{L'}_{K,-1}(5)]$$
$$+ \frac{2D}{\sqrt{2}}\begin{pmatrix} L & 2 & L' \\ -K & 0 & K \end{pmatrix}\begin{pmatrix} L & 2 & L' \\ -1 & 1 & 0 \end{pmatrix}[\bar{C}^{L'}_{K,0}(1) + \bar{C}^{L'}_{K,0}(2)]$$
$$- \frac{D}{\sqrt{2}}\begin{pmatrix} L & 2 & L' \\ -K & 0 & K \end{pmatrix}\begin{pmatrix} L & 2 & L' \\ -1 & -1 & 2 \end{pmatrix}[\bar{C}^{L'}_{K,2}(8) + \bar{C}^{L'}_{K,-2}(9)]$$
$$- iR_\perp[G^{L'}_{K,1}(4) - G^{L'}_{K,-1}(5)]\Big] = 0 \quad \text{(A4)}$$

$$[(\omega - \omega_0 - b) - i(T_2^{-1} + \tau_{L,1}^{-1})][\bar{C}^{L}_{K,1}(6) - \bar{C}^{L}_{K,-1}(7)]$$
$$+ \sum_{L'} N(LL')\Big[\Big(F - \frac{D'}{2}\Big)\begin{pmatrix} L & 2 & L' \\ -K & 0 & K \end{pmatrix}\begin{pmatrix} L & 2 & L' \\ -1 & 0 & 1 \end{pmatrix}[\bar{C}^{L'}_{K,1}(6) - \bar{C}^{L'}_{K,-1}(7)]$$
$$+ \frac{2D}{\sqrt{2}}\begin{pmatrix} L & 2 & L' \\ -K & 0 & K \end{pmatrix}\begin{pmatrix} L & 2 & L' \\ -1 & 1 & 0 \end{pmatrix}[\bar{C}^{L'}_{K,0}(2) + \bar{C}^{L'}_{K,0}(3)]$$
$$- \frac{D}{\sqrt{2}}\begin{pmatrix} L & 2 & L' \\ -K & 0 & K \end{pmatrix}\begin{pmatrix} L & 2 & L' \\ -1 & -1 & 2 \end{pmatrix}[\bar{C}^{L'}_{K,2}(8) + \bar{C}^{L'}_{K,-2}(9)]$$
$$- iR_\perp[G^{L'}_{K,1}(6) - G^{L'}_{K,-1}(7)]\Big] = 0 \quad \text{(A5)}$$

$$[(\omega - \omega_0) - i(T_2^{-1} + \tau_{L,2}^{-1})][\bar{C}^{L}_{K,2}(8) + \bar{C}^{L}_{K,-2}(9)]$$
$$- \sum_{L'} N(LL')\Big(F\begin{pmatrix} L & 2 & L' \\ -K & 0 & K \end{pmatrix}\begin{pmatrix} L & 2 & L' \\ -2 & 0 & 2 \end{pmatrix}[\bar{C}^{L'}_{K,2}(8) + \bar{C}^{L'}_{K,-2}(9)]$$
$$+ \frac{D}{\sqrt{2}}\begin{pmatrix} L & 2 & L' \\ -K & 0 & K \end{pmatrix}\begin{pmatrix} L & 2 & L' \\ -2 & 1 & 1 \end{pmatrix}\{[\bar{C}^{L'}_{K,1}(4) - \bar{C}^{L'}_{K,-1}(5)]$$
$$+ [\bar{C}^{L'}_{K,1}(6) - \bar{C}^{L'}_{K,-1}(7)]\} - iR_\perp[G^{L'}_{K,2}(8) + G^{L'}_{K,-2}(9)]\Big) = 0 \quad \text{(A6)}$$

Downloaded by [Tomsk State University of Control Systems and Radio] at 11:49 21 February 2013

where $\hbar\omega_0$ is electronic Zeeman splitting

$$N(LL') = \sqrt{(2L+1)(2L'+1)}$$

$$\tau_{L,M} = R_\perp L(L+1) + (R_\parallel - R_\perp)M^2$$

$$\bar{C}^L_{K,M} = \frac{1}{2}(C^L_{K,M} + C^L_{-K,M})$$

$$G^L_{K,M} = \sum_{L''=0,2,4} X^{L''}_{00}\begin{pmatrix} L & L'' & L' \\ -K & 0 & K \end{pmatrix}\begin{pmatrix} L & L'' & L' \\ -M & 0 & M \end{pmatrix}\bar{C}^{L'}_{K,M}(j)$$

$$X^0_{00} = \frac{2\lambda^2}{15}; \quad X^2_{00} = -2\lambda\left(1 - \frac{\lambda}{21}\right); \quad X^4_{00} = \frac{-8}{35}\lambda^2$$

$$X_j = \frac{\hbar\omega_j d_j}{2kT}; \quad d_j = \frac{1}{2}|\gamma_e| B_1$$

$$I_L = \int dx P_L(x)\exp(-\lambda x^2/2) \Big/ \iint\Big[\, dx \exp(-\lambda x^2)\Big]^{1/2}$$

$P_L(X)$ is Legendres Polynomial

$$F = \frac{2(g_\parallel - g_\perp)}{3}\beta_e B_0$$

$$b = -\frac{|\gamma_e|}{6}(a_\parallel + 2a_\perp)$$

$$D' = -\sqrt{\frac{8}{3}}D$$

$$D = -\frac{1}{\sqrt{6}}|\gamma_e|(a_\parallel - a_\perp)$$

Downloaded by [Tomsk State University of Control Systems and Radio] at 11:49 21 February 2013